Preprints of the 21st IFAC World Congress (Virtual)
Berlin, Germany, July 12-17, 2020

Asymmetric Barrier Lyapunov Function based Practical Fixed-time Control of Vertical Take-off/ Vertical Landing Reusable Launch Vehicles with Partial State Constraints

Xiaozhe Ju†. Feng Wang*. Changzhu Wei*. Liang Zhang***

**School of Astronautics, Harbin Institute of Technology, Harbin 150001, China*
*** School of Aeronautical and Astronautical, Sun Yat-sen University, Guangzhou 510275, China*
†Corresponding Author (E-mail: juhitnuaa@gmail.com)

Abstract: In order to stabilize the vertical take-off/ vertical landing reusable launch vehicles in aerodynamic guidance phase against complex disturbances and partial state constraints, an asymmetric logarithm-type barrier function and asymmetric double-exponential-type barrier function are proposed, where the latter is smooth with respect to system states and has a higher application value compared with the logarithm-type one. Based on the barrier functions and practical fixed-time control theory, two practical fixed-time control laws are derived to drive the attitude tracking errors to a small neighborhood of the origin within a fixed time and ensure the attitude constraints unviolated. Simulation results demonstrate the efficiency of the controllers.

Keywords: Vertical take-off/ vertical landing, aerodynamic guidance phase, partial state constraints, practical fixed-time, asymmetric logarithm-type barrier function, asymmetric double-exponential-type barrier function

1. INTRODUCTION

In the typical flight profile of vertical take-off/ vertical landing (VTVL) reusable launch vehicles (RLVs), aerodynamic guidance phase plays a significant role in successful and precise landing (C.Z. Wei, X.Z Ju, R. Wu, 2019). VTVL RLVs adjust attack angle and sideslip angle in this phase to utilize the pneumatic overload for position correction. Due to the strong couplings and external disturbances (Zhang L., Wei C., Wu R., Cui, N. 2018), the control system of VTVL RLVs requires high robustness.

Many advanced methods have been developed to stabilize flight vehicles, such as adaptive control (Xu B. 2015), sliding mode control (SMC) (An H., Wang C., Fi dan. 2017) and so on. However, due to slender structure, VTVL RLVs are more vulnerable to structural damage caused by aerodynamic overload than common flight vehicles. Hence the attack angle and sideslip angle should maintain within a specific range to prevent aerodynamic load from exceeding the limits (Blanchet P, Bartos, B. 2001). Therefore, the essential control problem is to stabilize RLVs against complex disturbances and guarantee the constraints unviolated, which makes the control of RLVs more difficult and challenging.

Barrier Lyapunov function (BLF) based control is efficient in addressing such complicated problems with rigorous constraints. This methodology utilizes barrier functions to ensure constraints unviolated (Tee K. P, Ge S S. 2012). The logarithm-type BLF (LBLF) was first used for Brunovsky systems (Ngo, Mahony, and Jiang 2005). After that, integral-type BLF (IBLF) was proposed for state constraints of strict feedback systems (Tee K. P, Ge S S. 2012). To achieve the trajectory tracking in the presence of output constraints, an asymmetric barrier integral-type function is employed (He W., Yin, Z., Sun C. 2016). Other applications of BLF can be found in An H., Xia H., Wang C. (2017) and so on. Although simulation results prove the effectiveness, system states converge in an exponential manner. Since a faster response is expected in the aerodynamic guidance phase, a fixed-time convergent controller should be developed.

Exponential-type BLF (EBLF) is a novel type of BLF, based on which Z.W Wang derived a fixed-time controller for bilateral teleoperation systems (Wang, Z., Liang B, Wang, X. 2018). Then a further research on EBLF was accomplished by Z.W. Wang for synchronization control with position error constraints (Wang, Z., Sun Y, Liang B. 2019). However, these two controllers are dedicated to deal with symmetric constraints, while the constraints on attack angle and sideslip angle are asymmetric given the asymmetric aerodynamic coefficients of VTVL RLVs.

Motivated by the aforementioned analysis, we propose two practical fixed-time convergent controllers based on asymmetric IBLF (AIBLF) and asymmetric double-exponential-type BLF (ADEBLF) respectively. The main contributions of this paper are as follows.

1) AIBLF and ADEBLF are proposed to deal with control problems with asymmetric constraints. ADEBLF is a smooth function and still works in the condition of infinite bound, therefore it has a higher value of application compared with AIBLF.
2) Two practical fixed-time controllers based on AIBLF and ADEBLF are proposed to guarantee the practical fixed-time convergence and maintain partial states within allowable ranges.
3) ‘Barrier function’ is used to guarantee the stability against the lumped disturbances instead of utilizing disturbance observers or adaptive laws, resulting in a control system with much simpler structure.

The remainder of this research is organized as follows. Sec.2 provides some definitions and useful lemmas as preliminaries for controller deduction. The control problem of VTVL RLVs is formulated in Sec.3, and the derivation process of two controllers is presented in Sec.4. Simulation results are given in Sec.5 to demonstrate the effectiveness of the developed controllers, which are followed by the conclusion in Sec.6.

2. PRELIMINARIES

Some definitions and useful lemmas are introduced here for controller design. Considering the following system:

$$\dot{\boldsymbol{x}}(t)=\boldsymbol{f}(\boldsymbol{x}(t)),\quad \boldsymbol{x}(t_0)=\boldsymbol{x}_0 \tag{1}$$

where $\boldsymbol{x}\in\mathbb{R}^n$ is the state vector, $\boldsymbol{f}\in\mathbb{R}^n$ represents the vector field, which is piecewise continuous and Lipschitz in $\boldsymbol{x}$.

Definition 1 *(He W, Dong Y, Sun C. 2015) (Practical FxTC)* System (1) is said to be uniformly finite-time convergent to a vicinity $\boldsymbol{S}\subset\mathbb{R}^n$ of the origin, if for any initial conditions $\boldsymbol{x}_0\in\mathbb{R}^n$, there exists T such that the system state $\boldsymbol{x}(t)\in\boldsymbol{S}$ for all $t>T$. If T can be explicitly bounded by $T_{\max}$, $0\le T_{\max}<+\infty$, then the system is called practical fixed-time convergent to a vicinity of the origin.

Lemma 1 *(Tee K. P., Ge S. S., Tay E. H. 2009)* For any positive constants k_a, k_b, let $\hbar:=\{x\in\mathbb{R}:-k_a<x<k_b\}\subset\mathbb{R}$. Suppose there exist two functions $U:\mathbb{R}^l\times\mathbb{R}^+\to\mathbb{R}^+$ and $V_1:\hbar\to\mathbb{R}^+$, which are continuously differentiable and positive definite in their respective domains, such that

$$\begin{aligned}&V_1(x)\to\infty \text{ as } x\to -k_a \text{ or } x\to k_b\\ &\gamma_1(\|\omega\|)\le U(\omega)\le\gamma_2(\|\omega\|)\end{aligned} \tag{2}$$

where γ_1 and γ_2 are class K_∞ functions. Let $V(x,\omega)=V_1(x)+U(\omega)$ and $x(0)\in\hbar\in(-k_a,k_b)$. If:

$$\partial V/\partial t\le-\mu V+\lambda \tag{3}$$

where μ and λ are positive constants, then $x(t)$ remains in the open set $x\in(-k_a,k_b)$, $\forall t\in[0,+\infty)$.

Lemma 2 *(Jiang B., Hu Q., Friswell M. I. 2016):* Consider the system (1). Suppose there exists a positive continuous-derivable function $V:\mathbb{R}^n\to\mathbb{R}_+$ such that

$$\dot{V}(\boldsymbol{x})\le-\alpha V^p(\boldsymbol{x})-\beta V^g(\boldsymbol{x})+\theta \tag{4}$$

where $p<1$, $g<1$, θ, α and $\beta>0$. Then the system is practical fixed-time stable. The settling time T and convergence neighbourhood D_0 can be represented as

$$\begin{aligned}&T\le\frac{1}{\alpha(1-p)}+\frac{1}{\beta(g-1)}\\ &D_0=\left\{\lim_{t\to T}\boldsymbol{x}\,|\,V(\boldsymbol{x})\le\min\left[\alpha^{-\frac{1}{p}}\left(\frac{\theta}{1-\zeta}\right)^{\frac{1}{p}},\beta^{-\frac{1}{p}}\left(\frac{\theta}{1-\zeta}\right)^{\frac{1}{g}}\right]\right\}\end{aligned} \tag{5}$$

where $0<\zeta\le1$.

Lemma 3 *(Wang Z., Sun Y., Liang, B. 2019):* Denote $\mathrm{sig}(x,p)=\mathrm{sgn}(x)|x|^p$. If $p_1>0$ and $0<p_2\le1$, $\forall x,y\in\mathbb{R}$, then

$$|\mathrm{sig}(x,p_1p_2)-\mathrm{sig}(y,p_1p_2)|\le2^{1-p_2}|\mathrm{sig}(x,p_1)-\mathrm{sig}(y,p_1)|^{p_2} \tag{6}$$

Lemma 4 *(Wang, Z., Sun, Y., Liang, B. 2019):* If c, $d>0$ and $\gamma>0$, we have

$$\frac{c}{c+d}\gamma|x|^{c+d}+\frac{d}{c+d}\gamma^{-\frac{c}{d}}|y|^{c+d}\ge|x|^c|y|^d \tag{7}$$

Lemma 5 *(Tee, K. P., Ge, S. S. 2012):* Consider the function:

$$V(z,\alpha)=\int_0^z\frac{\sigma k_c^2}{k_c^2-(\sigma+\alpha)^2}\mathrm{d}\sigma \tag{8}$$

where $z=x-\alpha$, $|\alpha|<k_c$. $V(z,\alpha)\le k_c^2z^2/(k_c^2-x^2)$, $\forall|x|<k_c$.

Lemma 6 *(Zhang L., Wei C., Wu R., Cui, N. 2018):* If $v\in\mathbb{R}^+$ and $v>1$, then for any $x,y\in\mathbb{R}$, we have $|x+y|^v\le2^{v-1}|x^v+y^v|$.

3. PROBLEM FORMULATION

Along the deduction lines in Zhang L., Wei C., Wu R., Cui, N.(2018), the nominal control-oriented model of VTVL RLVs can be described as follows.

$$\begin{cases}\dot{\boldsymbol{\Omega}}=\boldsymbol{R\omega}+\Delta\boldsymbol{f}\\ \dot{\boldsymbol{\omega}}=-\boldsymbol{J}^{-1}\boldsymbol{\omega}^{\times}\boldsymbol{J\omega}+\boldsymbol{J}^{-1}\boldsymbol{B}_1\boldsymbol{U}+\boldsymbol{J}^{-1}\Delta\boldsymbol{d}\end{cases} \tag{9}$$

where $\boldsymbol{\omega}=[p\quad q\quad r]^{\mathrm{T}}$ is the attitude angular velocity vector, $\boldsymbol{\Omega}=[\alpha\quad\beta\quad\sigma]^{\mathrm{T}}$ is the attitude vector. $\Delta\boldsymbol{d}$ and $\Delta\boldsymbol{f}$ means the unknown bounded disturbance vector. $\boldsymbol{\omega}^{\times}$ represents the skew-symmetric matrix operator on vector $\boldsymbol{\omega}$, $\boldsymbol{J}$ is the inertia matrix, $\boldsymbol{B}_1$ and $\boldsymbol{R}$ are respectively the control moment matrix and the coordinate transformation matrix, of which detailed forms can be found in Zhang L., Wei C., Wu R. (2018). Considering uncertainties of rotational inertia and aerodynamic coefficients, the system (9) is converted to

$$\begin{cases}\dot{\boldsymbol{x}}_1=\boldsymbol{x}_2+\Delta\boldsymbol{f}\\ \dot{\boldsymbol{x}}_2=\boldsymbol{M}+\varsigma(t)+\boldsymbol{v}(t)\end{cases} \tag{10}$$

where $\boldsymbol{x}_1=\boldsymbol{\Omega}$, $\boldsymbol{x}_2=\boldsymbol{R\omega}$, $\boldsymbol{v}(t)=-\boldsymbol{RJ}^{-1}\boldsymbol{\omega}^{\times}\boldsymbol{J\omega}$, $\boldsymbol{M}=\boldsymbol{RJ}^{-1}\boldsymbol{B}_1\boldsymbol{U}$, and:

$$\varsigma(t)=-\boldsymbol{R}(\boldsymbol{J}+\Delta\boldsymbol{J})^{-1}\left((\boldsymbol{B}_1+\Delta\boldsymbol{B}_1)\boldsymbol{U}+\Delta\boldsymbol{d}-\boldsymbol{\omega}^{\times}(\boldsymbol{J}+\Delta\boldsymbol{J})\boldsymbol{\omega}\right)-\boldsymbol{RJ}^{-1}\boldsymbol{B}_1\boldsymbol{U} \tag{11}$$

where $\Delta\boldsymbol{J}$ and $\Delta\boldsymbol{B}_1$ denote the uncertain parts of $\boldsymbol{J}$ and $\boldsymbol{B}_1$.

Denote the reference signals as $\boldsymbol{y}_d=[y_{d1}\quad y_{d2}\quad y_{d3}]^{\mathrm{T}}$, where y_{d1}, y_{d2} and y_{d3} are attitude orders in roll, yaw and pitch channels. Here give assumptions for the deduction.

Assumption 1 There exist constants ι such that $\|\varsigma(t)\|<\iota$, i.e. disturbances $\varsigma(t)$ are bounded.

Assumption 2 There exists a constant κ such that $\|\dot{\boldsymbol{y}}_d-\Delta\boldsymbol{f}\|<\kappa$, i.e. $\boldsymbol{y}_d$ satisfy the Lipschtiz condition.

The main objective is to design the control law $\boldsymbol{U}$ such that: 1) Both $\boldsymbol{x}_1(t)-\boldsymbol{y}_d$ and $\boldsymbol{x}_2(t)$ converge to a small neighbourhood of the origin in a fixed time in spite of couplings and uncertainties. 2) During the convergence process, states $\boldsymbol{x}_1(t)$ don't violate the constraints as follows:

$$-k_{ai}<x_{1i}<k_{bi}\ \ for\ x_{1i}\in\boldsymbol{x}_1,\ \forall t\ge0 \tag{12}$$

where k_{ai} and k_{bi} are specified positive values.

4. CONTROLLER DESIGN

In this section, two practical fixed-time controllers are proposed respectively dependent on AIBLF and ADEBLF. Both controllers achieve the practical fixed-time convergence, while the application field and continuity of the ADEBLF-based controller is better than the AIBLF-based controller.

4.1 Asymmetric Integral Barrier Lyapunov function based Practical Fixed-time Control

We first give a control law as follows:

$$\boldsymbol{U}=\left(\boldsymbol{RJ}^{-1}\boldsymbol{B}_1\right)^{-1}[M_1,M_2,M_3]^{\mathrm{T}} \tag{13}$$

where

$$M_i=\begin{pmatrix}-\nu_i-\dfrac{1}{k_{ci}^2(t)-z_{2i}^2}\operatorname{sgn}(z_{2i})-\operatorname{sig}(z_{2i})^{\frac{2q_1}{p_1}-1}\\ -\operatorname{sig}(z_{2i})^{\frac{2q_2}{p_2}-1}-\dfrac{\Lambda_{1i}k_{ai}^2}{2k_{ai}^2-2x_{1i}^2}-\dfrac{(1-\Lambda_{1i})k_{bi}^2}{2k_{bi}^2-2x_{1i}^2}\end{pmatrix}\; z_{1i}=x_{1i}-y_{di}\;\Lambda_1=\begin{cases}0 & x_{1i}>0\\ 1 & x_{1i}\le 0\end{cases}$$

$$z_{2i}=x_{2i}+\phi(x_{1i},z_{1i})-\left(\Lambda_{1i}\frac{k_{ai}^2-x_{1i}^2}{k_{ai}^2}+(1-\Lambda_{1i})\frac{k_{bi}^2-x_{1i}^2}{k_{bi}^2}\right)\frac{\kappa z_{1i}^2\rho_1}{\varepsilon_0}\operatorname{sgn}(z_{1i})$$

$\phi(x_{1i},z_{1i})$ and $k_{ci}(t)$ are specified functions which will be illustrated in the following part. ε_0 is a positive coefficient. Both $q_1/p_1>1$ and $1>q_2/p_2>0.5$ hold.

Theorem 1*:* With the controller (13), the system (10) has the following properties: 1) $\boldsymbol{x}_1(t)-\boldsymbol{y}_d$ converge into a small neighbourhood of the origin within a fixed time. 2) The predefined constraints $-k_{ai}<x_{1i}<k_{bi}$ will not be violated during the convergence process.

Proof Consider a Lyapunov candidate function:

$$V_1(z,\alpha)=\sum_{i=1}^{3}V_{1i}+\sum_{i=1}^{3}V_{2i}\qquad V_{2i}=z_{2i}^2$$
$$V_{1i}=\Lambda_{1i}\int_0^{z_{1i}}\frac{\sigma k_{ai}^2}{k_{ai}^2-(\sigma_i+\alpha_{0i})^2}\mathrm{d}\sigma_i+(1-\Lambda_{1i})\int_0^{z_{1i}}\frac{\sigma k_{bi}^2}{k_{bi}^2-(\sigma_i+\alpha_{0i})^2}\mathrm{d}\sigma_i \tag{14}$$

where $z_{1i}=x_{1i}-\alpha_{0i}$, $\alpha_{0i}=y_{di}$, $-k_{bi}<-A_{1i}\le\alpha_{0i}\le A_{0i}<k_{ai}$ holds for $A_{ji}\in\mathbb{R}_+$, $j=1,2$, $z_{2i}=x_{2i}-\alpha_{1i}$, α_{1i} is the stabilizing function of z_{1i} . V_1 is a positive definite, piecewise differentiable function which becomes infinite if x_{1i} approaches $-k_{ai}$ and k_{bi} .

Step 1: Based on Lemma 5, the functional V_{1i} satisfies

$$V_{1i}\le\Lambda_{1i}\frac{k_{ai}^2z_{1i}^2}{k_{ai}^2-x_{1i}^2}+(1-\Lambda_{1i})\frac{k_{bi}^2z_{1i}^2}{k_{bi}^2-x_{1i}^2} \tag{15}$$

If $z_{1i}\ne 0$, then the time-derivative of V_{1i} is given by

$$\begin{aligned}\dot V_{1i}(z_{1i},\alpha_{0i})&=\Lambda_{1i}\frac{k_{ai}^2z_{1i}}{k_{ai}^2-x_{1i}^2}(z_{2i}+\alpha_{1i}+\Delta f_i-\dot y_{di})+\\&(1-\Lambda_{1i})\frac{k_{bi}^2z_{1i}}{k_{bi}^2-x_{1i}^2}(z_{2i}+\alpha_{1i}+\Delta f_i-\dot y_{di})+\frac{\partial V_{1i}}{\partial y_{di}}\dot y_{di}\end{aligned} \tag{16}$$

Via integration by parts and substitution $\sigma_i=\beta_iz_{1i}$, we have:

$$\frac{\partial V_{1i}}{\partial y_{di}}=\Lambda_{1i}z_{1i}\left(\frac{k_{ai}^2}{k_{ai}^2-x_{1i}^2}-\rho_1(z_{1i},y_{di})\right)+(1-\Lambda_{1i})z_{1i}\left(\frac{k_{bi}^2}{k_{bi}^2-x_{1i}^2}-\rho_1(z_{1i},y_{di})\right) \tag{17}$$

$$\begin{aligned}\rho_1(z_{1i},y_{di})&=\Lambda_{1i}\frac{k_{ai}}{2z_{1i}}\ln\frac{(k_{ai}+z_{1i}+y_{di})(k_{ai}-y_{di})}{(k_{ai}-z_{1i}-y_{di})(k_{ai}+y_{di})}\\&+(1-\Lambda_{1i})\frac{k_{bi}}{2z_{1i}}\ln\frac{(k_{bi}+z_{1i}+y_{di})(k_{bi}-y_{di})}{(k_{bi}-z_{1i}-y_{di})(k_{bi}+y_{di})}\end{aligned} \tag{18}$$

With the use of L'Hôpital's rule, it can be derived that

$$\begin{aligned}\lim_{z_{1i}\to 0_+}\rho_{1i}(z_{1i},y_{di})&=\lim_{z_{1i}\to 0_+}\frac{k_{ai}^2}{k_{ai}^2-(z_{1i}+y_{di})^2}=\frac{k_{ai}^2}{k_{ai}^2-y_{di}^2}\\ \lim_{z_{1i}\to 0_-}\rho_{1i}(z_{1i},y_{di})&=\lim_{z_{1i}\to 0_-}\frac{k_{bi}^2}{k_{bi}^2-(z_{1i}+y_{di})^2}=\frac{k_{bi}^2}{k_{bi}^2-y_{di}^2}\end{aligned} \tag{19}$$

Given that $-k_{ai}<y_{di}<k_{bi}$, according to Assumption 1, $\rho_1(z_{1i},y_{di})$ is well-defined in the neighbourhood of $z_{1i}=0$.

Design the stabilizing function α_{i1} as follows

$$\alpha_{i1}=-\phi(x_{1i},z_{1i})+\left(\Lambda_{1i}\frac{k_{ai}^2-x_{1i}^2}{k_{ai}^2}+(1-\Lambda_{1i})\frac{k_{bi}^2-x_{1i}^2}{k_{bi}^2}\right)\frac{\kappa z_{1i}^2\rho_1}{\varepsilon_0}\operatorname{sgn}(z_{1i})$$
$$\phi(x_{1i},z_{1i})=\begin{cases}\left(\Lambda_{1i}\dfrac{k_{ai}^2-x_{1i}^2}{k_{ai}^2z_{1i}}+(1-\Lambda_{1i})\dfrac{k_{bi}^2-x_{1i}^2}{k_{bi}^2z_{1i}}\right)\left(k_{1i}\upsilon_{1i}^{\frac{q_1}{p_1}}+k_{1i}\upsilon_{1i}^{\frac{q_2}{p_2}}\right) & z_{i1}\ne 0\\ 0 & z_{1i}=0\end{cases} \tag{20}$$

$$\upsilon_{1i}=\Lambda_{1i}\frac{k_{ai}^2z_{1i}^2}{k_{ai}^2-x_{1i}^2}+(1-\Lambda_{1i})\frac{k_{bi}^2z_{1i}^2}{k_{bi}^2-x_{1i}^2} \tag{21}$$

where ε_0 is a small positive constant such that $|\varepsilon_{0i}|\in\min\{k_{ai},k_{bi}\}$, and $k_{1i}>0$ determining the convergence rate. Considering that $\lim_{z_{1i}\to 0}\phi(x_{1i},z_{1i})=\phi(x_{1i},0)=0$, $\phi(x_{1i},z_{1i})$ is a continuous function.

Substituting (20) into (16) yields:

$$\begin{aligned}\dot V_{1i}(z_{1i},\alpha_{0i})&=-\left(k_{1i}\upsilon_{1i}^{\frac{q_1}{p_1}}+k_{1i}\upsilon_{1i}^{\frac{q_2}{p_2}}\right)+\Lambda_{1i}\frac{k_{ai}^2z_{2i}}{k_{ai}^2-x_{1i}^2}+(1-\Lambda_{1i})\frac{k_{bi}^2z_{2i}}{k_{bi}^2-x_{1i}^2}\\&+\left(\Lambda_{1i}\frac{k_{ai}^2-x_{1i}^2}{k_{ai}^2}+(1-\Lambda_{1i})\frac{k_{bi}^2-x_{1i}^2}{k_{bi}^2}\right)\frac{\kappa z_{1i}\rho_1}{\varepsilon_0}\operatorname{sgn}(z_{1i})\\&-\left(\Lambda_{1i}\frac{k_{ai}^2-x_{1i}^2}{k_{ai}^2}+(1-\Lambda_{1i})\frac{k_{bi}^2-x_{1i}^2}{k_{bi}^2}\right)\rho_1\dot y_d,\; z_{1i}\ne 0\end{aligned} \tag{22}$$

Step 2: Based on (10), the time-derivative of V_{2i} is

$$\dot V_{2i}=2z_{2i}(\varsigma_i+\nu_i+M_i-\dot\alpha_{1i}) \tag{23}$$

where $\dot\alpha_{1i}$ exists if z_{i1} doesn't equal to zero.

Design the stabilizing function as:

$$M_i=\begin{pmatrix}-\nu_i-\dfrac{1}{k_{ci}^2(t)-z_{2i}^2}\operatorname{sgn}(z_{2i})-\operatorname{sig}(z_{2i})^{\frac{2q_1}{p_1}-1}-\operatorname{sig}(z_{2i})^{\frac{2q_2}{p_2}-1}\\ -\dfrac{\Lambda_{1i}k_{ai}^2}{2k_{ai}^2-2x_{1i}^2}-\dfrac{(1-\Lambda_{1i})k_{bi}^2}{2k_{bi}^2-2x_{1i}^2}\end{pmatrix} \tag{24}$$

where $|k_{ci}(t)|$ is a decreasing function, $|k_{ci}(0)|>|z_{2i}(0)|$ and $\{|k_{ci}(t)|<\zeta\mid t>t_1,\zeta\in\mathbb{R}_+\ll 1\}$. Here, $1/(k_{ci}^2(t)-z_{2i}^2)$ is exactly a barrier function that it grows infinity if z_{2i} approaches $k_{ci}(t)$.

Substituting (24) into (23) yields

$$\dot V_{2i}=2z_{2i}\begin{pmatrix}-\dfrac{1}{k_{ci}^2(t)-z_{2i}^2}\operatorname{sgn}(z_{2i})-\operatorname{sig}(z_{2i})^{\frac{2q_1}{p_1}-1}\\ -\operatorname{sig}(z_{2i})^{\frac{2q_2}{p_2}-1}-\dot\alpha_{1i}-\dfrac{\Lambda_{1i}k_{ai}^2}{2k_{ai}^2-2x_{1i}^2}-\dfrac{(1-\Lambda_{1i})k_{bi}^2}{2k_{bi}^2-2x_{1i}^2}\end{pmatrix} \tag{25}$$

Step 3: Based on (22) and (25), we obtain the time-derivative of the Lyapunov function candidate $V_1(z,\alpha)$ as follows

$$\dot V_1=\sum_{i=1}^{3}\dot V_{1i}+\sum_{i=1}^{3}\dot V_{2i}\le -2^{5-\frac{5q_1}{p_1}}\Xi V_1^{\frac{q_1}{p_1}}-2^{5-\frac{5q_2}{p_2}}\Xi V_1^{\frac{q_2}{p_2}}+\theta \tag{26}$$

where $\Xi=\min\{k_{1i},2\}$, and

$$\theta=\sum_{i=1}^{3}\begin{pmatrix}-\left(\Lambda_{1i}\dfrac{k_{ai}^2-x_{1i}^2}{k_{ai}^2}+(1-\Lambda_{1i})\dfrac{k_{bi}^2-x_{1i}^2}{k_{bi}^2}\right)\rho_1\dot y_d+2z_{2i}\left(-\dfrac{1}{k_{ci}^2(t)-z_{2i}^2}\operatorname{sgn}(z_{2i})-\dot\alpha_{1i}\right)\\ -\left(\Lambda_{1i}\dfrac{k_{ai}^2-x_{1i}^2}{k_{ai}^2}+(1-\Lambda_{1i})\dfrac{k_{bi}^2-x_{1i}^2}{k_{bi}^2}\right)\dfrac{\kappa z_{1i}\rho_1}{\varepsilon_0}\operatorname{sgn}(z_{1i})\end{pmatrix}$$

For ease of derivation, four regions are introduced here:

$$\begin{aligned}\boldsymbol{\Omega}_1&=\left\{\{z_{1i},z_{2i}\}\mid |z_{1i}|\ge\varepsilon_0,|z_{2i}|\ge\sqrt{\left(k_{ci}^2(t)-\min\left\{\frac{1}{|\dot\alpha_{1i}|},k_{ci}^2\right\}\right)}\right\}\\ \boldsymbol{\Omega}_2&=\left\{\{z_{1i},z_{2i}\}\mid |z_{1i}|\ge\varepsilon_0,|z_{2i}|\le\sqrt{\left(k_{ci}^2(t)-\min\left\{\frac{1}{|\dot\alpha_{1i}|},k_{ci}^2\right\}\right)}\right\}\\ \boldsymbol{\Omega}_3&=\left\{\{z_{1i},z_{2i}\}\mid |z_{1i}|\le\varepsilon_0,|z_{2i}|\ge\sqrt{\left(k_{ci}^2(t)-\min\left\{\frac{1}{|\dot\alpha_{1i}|},k_{ci}^2\right\}\right)}\right\}\\ \boldsymbol{\Omega}_4&=\left\{\{z_{1i},z_{2i}\}\mid |z_{1i}|\le\varepsilon_0,|z_{2i}|\le\sqrt{\left(k_{ci}^2(t)-\min\left\{\frac{1}{|\dot\alpha_{1i}|},k_{ci}^2\right\}\right)}\right\}\end{aligned} \tag{27}$$

If $\{z_{1i}(0), z_{2i}(0)\} \in \boldsymbol{\Omega}_1$, then $\theta < 0$ and we have

$$\dot{V}_1 \le \sum_{i=1}^{3}\left(-\Phi\left(V_{1i}^{\frac{q_1}{p_1}} + V_{1i}^{\frac{q_2}{p_2}}\right) - \Phi\left(V_{2i}^{\frac{q_1}{p_1}} + V_{2i}^{\frac{q_2}{p_2}}\right)\right) \le -2^{5-\frac{5q_1}{p_1}}\Phi V_1^{\frac{q_1}{p_1}} - 2^{5-\frac{5q_2}{p_2}}\Phi V_1^{\frac{q_2}{p_2}} \tag{28}$$

where $\Phi = \min\{2, k_{11}, k_{12}, k_{13}\}$. According to Lemma 2, $\{z_{1i}, z_{2i}\}$ will move across region $\boldsymbol{\Omega}_1$ into $\boldsymbol{\Omega}_2$, $\boldsymbol{\Omega}_3$ or $\boldsymbol{\Omega}_4$ within T_1, where $T_1 \le \dfrac{1}{2^{5-5q_1/p_1}\Xi(1-q_1/p_1)} + \dfrac{1}{2^{5-5q_2/p_2}(q_2/p_2-1)}$.

If $\{z_{1i}, z_{2i}\}$ moves into $\boldsymbol{\Omega}_2$, then

$$\dot{V}_{1i}(z_{1i}, \alpha_{0i}) \le -\left(k_{1i}\upsilon_{1i}^{\frac{q_1}{p_1}} + k_{1i}\upsilon_{1i}^{\frac{q_2}{p_2}}\right) + \theta_{i1} \tag{29}$$

where:

$$\theta_{i1} = \Lambda_{1i}k_{ai}^2\sqrt{\left(k_{ci}^2 - \min\left\{\frac{1}{|\dot{\alpha}_{1i}|}, k_{ci}^2\right\}\right)}\Big/\left(k_{ai}^2 - x_{1i}^2\right) + (1-\Lambda_{1i})k_{bi}^2\sqrt{\left(k_{ci}^2 - \min\left\{\frac{1}{|\dot{\alpha}_{1i}|}, k_{ci}^2\right\}\right)}\Big/\left(k_{bi}^2 - x_{1i}^2\right)$$

Thus $\{z_{1i}, z_{2i}\}$ will converge into the region $\boldsymbol{D}_1$ within T_2, where $T_2 \le \dfrac{1}{k_{1i}(1-q_1/p_1)} + \dfrac{1}{k_{1i}(q_2/p_2-1)}$ and

$$\boldsymbol{D}_1 = \left\{\begin{array}{l} \{z_{1i}, z_{2i}\} \mid V_{1i}(z_{1i}) \le \min\left[k_{1i}^{-\frac{p_1}{q_1}}\left(\theta_{i1}/(1-\varsigma)\right)^{\frac{p_1}{q_1}}, k_{1i}^{-\frac{p_2}{q_2}}\left(\theta_{i1}/(1-\varsigma)\right)^{\frac{p_2}{q_2}}\right] \\ |z_{2i}| < \sqrt{\left(k_{ci}^2 - \min\left\{\frac{1}{|\dot{\alpha}_{1i}|}, k_{ci}^2\right\}\right)} \end{array}\right.$$

If $\{z_{1i}, z_{2i}\}$ moves into $\boldsymbol{\Omega}_3$, then $\{z_{1i}, z_{2i}\}$ will converge into the region $\boldsymbol{D}_2$ within t_1, where

$$\boldsymbol{D}_2 = \left\{\{z_{1i}, z_{2i}\} \mid |z_{1i}| \le \varepsilon_0,\ |z_{2i}| < \zeta\right\} \tag{30}$$

Based on the abovementioned analysis, $\{z_{1i}, z_{2i}\}$ with any initial values can converge into the region $\boldsymbol{D}_3$ within T_3, where $\boldsymbol{D}_3 = \boldsymbol{\Omega}_4 \cup \boldsymbol{D}_1 \cup \boldsymbol{D}_2$ and $T_3 \le \max\{t_1 + T_1, T_2 + T_1\}$. Moreover, constraints $-k_{ai} < x_{1i} < k_{bi}$ aren't violated.

4.2 Asymmetric Double-exponential Barrier Lyapunov function based Practical Fixed-time Control

As can be seen in (14), the AIBLF is not continuously differentiable at $z_{1i} = 0$. In order to get rid of discontinuity, an ADEBLF is proposed, which is inspired by Wang, Z., Liang, B., Wang, X. (2018). Furthermore, a practical fixed-time control law is deduced based on the proposed novel BLF. The boundaries of tracking errors are set as $\delta_a = k_{ai} - y_{di\_\min}$ and $\delta_b = k_{bi} - y_{di\_\max}$, where $(y_{di\_\min}, y_{di\_\max})$ are the limits of reference orders in three channels. Via redefining the states $\boldsymbol{x}_1(t) = \boldsymbol{\Omega}(t) - \boldsymbol{y}_d(t)$ and $\boldsymbol{x}_2(t) = \boldsymbol{R\omega}(t)$, a converted model is derived as follows

$$\dot{\boldsymbol{x}}_1(t) = \boldsymbol{x}_2(t) + \boldsymbol{F}(t),\ \dot{\boldsymbol{x}}_2(t) = \boldsymbol{M} + \varsigma(t) + \boldsymbol{v}(t) \tag{31}$$

where $\boldsymbol{F}(t) = -\dot{\boldsymbol{y}}_d(t)$, $\boldsymbol{v}(t) = -\boldsymbol{RJ}^{-1}\boldsymbol{\omega}^{\times}\boldsymbol{J\omega}$, $\boldsymbol{M} = \boldsymbol{RJ}^{-1}\boldsymbol{B}_1\boldsymbol{U}$ and

$$\begin{aligned} \varsigma(t) = &-\boldsymbol{R}(\boldsymbol{J}+\Delta\boldsymbol{J})^{-1}\boldsymbol{\omega}^{\times}(\boldsymbol{J}+\Delta\boldsymbol{J})\boldsymbol{\omega} + (\boldsymbol{J}+\Delta\boldsymbol{J})^{-1}\Delta\boldsymbol{d}(t) \\ &+ \boldsymbol{R}(\boldsymbol{J}+\Delta\boldsymbol{J})^{-1}\left((\boldsymbol{B}_1 + \Delta\boldsymbol{B}_1)\boldsymbol{U} + \Delta\boldsymbol{d}\right) - \boldsymbol{v}(t) - \boldsymbol{RJ}^{-1}\boldsymbol{BU} \end{aligned} \tag{32}$$

The form of ADEBLF is given by:

$$\begin{aligned} &\Xi(\delta_a, \delta_b, x_1) = \frac{r_1\Upsilon(\delta_a, \delta_b)}{2r_3 + r_2}\left[\exp\left(\hat{x}_1/(\bar{x}_1 + \bar{\delta}_a)\right) + \exp\left(\hat{x}_1/(\bar{\delta}_b - \bar{x}_1)\right) - 2\right] \\ &\Upsilon(\delta_a, \delta_b) = (\delta_a + \delta_b)^{(2r_3+r_2)/r_1} \quad \bar{x}_1 = \mathrm{sig}(x)^{(2r_3+r_2)/r_1} \quad \hat{x}_1 = (|x|)^{(2r_3+r_2)/r_1} \\ &\bar{\delta}_a = \mathrm{sig}(\delta_a)^{(2r_3+r_2)/r_1} \quad \bar{\delta}_b = \mathrm{sig}(\delta_b)^{(2r_3+r_2)/r_1} \quad r_3 \ge r_4 \ge r_1 = 2r_2 > 0 \end{aligned} \tag{33, 34}$$

***Remark 1**:* The proposed ADEBLF is inspired by the EBLF in Wang Z., Liang B., Wang X. (2018). However, given the asymmetric constraints on the attack angle of VTVL RLVs, the EBLF is not suitable for use. Here the ADEBLF $\Xi(\delta_a, \delta_b, x_1)$ approaches infinity if $x_1 \to -\delta_a$ or $x_1 \to \delta_b$, thus it has a larger application field compared with the EBLF.

***Theorem 2**:* Consider a control law as follows

$$\boldsymbol{U} = \left(\boldsymbol{RJ}^{-1}\boldsymbol{B}_1\right)^{-1}[M_1, M_2, M_3]^{\mathrm{T}} \tag{35}$$

where

$$\begin{aligned} M_i = &-v_i(t) - \frac{1}{|\xi_{i1k}| - \varepsilon_2(t)} - \rho_0\xi_{i2k} - \frac{1}{2}\mathrm{sig}(\xi_{i2k})^{\frac{2r_3}{r_4}} \\ &-(\rho_{i6} + \rho_0)\mathrm{sgn}(\xi_{i2k}) - \rho_0\psi(\xi_{i2k})|\xi_{i2k}|^{-\frac{2r_3}{r_4}}\left(|\xi_{i1k}|^{\frac{2r_3+r_4}{r_4}} + |\xi_{i2k}|^{\frac{2r_3+r_4}{r_4}}\right)\mathrm{sgn}(\xi_{i2k}) \end{aligned} \tag{36}$$

where $\varepsilon_2(t)$ is a positive decreasing function, $\varepsilon_2(0) > \xi_{i1k}(0)$ and $\varepsilon_2(t_2) < \varepsilon_3$, $t_2 > 0$, $0 < \varepsilon_3 \ll 1$, $\psi(\xi_{i2k}) = \sin\left(\pi|\xi_{i2k}|^{2r_3/r_4}/2\varepsilon_1^{2r_3/r_4}\right)$ holds if $|\xi_{i2k}| < \varepsilon_1$, and $\psi(\xi_{i2k}) = 1$ if $|\xi_{i2k}| \ge \varepsilon_1$. $\rho_0 > 0$, $\rho_{i6} > 0$, ρ_{i6}, ξ_{i1k} and ξ_{i2k} are will be defined in the following part.

With the control law (36), the system (10) has the following properties: 1) $\boldsymbol{x}_1(t)$ converge into a small neighbourhood of the origin within a fixed time. 2) The predefined constraints $-\delta_{ai} < x_i < \delta_{bi}$ will not be violated.

***Proof**:* The candidate Lyapunov function for the closed-loop system is given by $V = V_1 + V_2$, $V_1 = \sum_{i=1,2,3}\Xi(\delta_a, \delta_b, x_1)$ and $V_2 = \sum_{i=1,2,3}\int_{x_{i2k}^*}^{x_{i2k}}\mathrm{sig}\left(\mathrm{sig}(\tau)^{r_4/r_2} - \mathrm{sig}(x_{i2k}^*)^{r_4/r_2}\right)^{2r_3/r_4}\mathrm{d}\tau$.

***Step 1**:* Taking the derivative of V_1 yields

$$\dot{V}_1 = \sum_{i=1,2,3}\left(\Upsilon(\delta_a, \delta_b)E_{ik}\mathrm{sig}(x_{i1})^{\frac{2r_3-r_2}{r_1}}\left(\frac{\bar{\delta}_{ia}}{(\bar{x}_{i1} + \bar{\delta}_{ia})^2} + \frac{\bar{\delta}_{ib}}{(\bar{\delta}_{ib} - \bar{x}_{i1})^2}\right)\begin{pmatrix} x_{i2k} - x_{i2k}^* \\ +x_{i2k}^* + F_i \end{pmatrix}\right) \tag{37}$$

where $E_{ik} = \exp\left(\hat{x}_{i1}/(\bar{x}_{i1} + \bar{\delta}_{ia})\right) + \exp\left(\hat{x}_{i1}/(\bar{\delta}_{ib} - \bar{x}_{i1})\right)$.

Via denoting $\xi_{i1k} = \mathrm{sig}(x_{i1})^{r_4/r_1}$, $x_{i2k}^* = -\kappa\,\mathrm{sgn}(\xi_{i1k}) - \alpha_0\mathrm{sig}(\xi_{i1k})^{r_2/r_4}$, $\alpha_0 > 0$, we have:

$$\begin{aligned} &\dot{V}_1 \le \Upsilon(\delta_a, \delta_b)\left(\sum_{i=1,2,3}V_{i11} - \sum_{i=1,2,3}V_{i12}\right) \\ &V_{i11} = E_{ik}\mathrm{sig}(x_{i1})^{\frac{2r_3-r_2}{r_1}}\left(\frac{\bar{\delta}_a}{(\bar{x}_{i1} + \bar{\delta}_{ia})^2} + \frac{\bar{\delta}_b}{(\bar{\delta}_{ib} - \bar{x}_{i1})^2}\right)(x_{i2k} - x_{i2k}^*) \\ &V_{i12} = \alpha_0E_{ik}\mathrm{sig}(\xi_{i1k})^{\frac{r_2}{r_4}}\mathrm{sig}(x_{i1})^{\frac{2r_3-r_2}{r_1}}\left(\frac{\bar{\delta}_{ia}}{(\bar{x}_{i1} + \bar{\delta}_{ia})^2} + \frac{\bar{\delta}_{ib}}{(\bar{\delta}_{ib} - \bar{x}_{i1})^2}\right) \end{aligned} \tag{38}$$

Denote $\xi_{i2k} = \mathrm{sig}(x_{i2k})^{r_4/r_2} - \mathrm{sig}(x_{i2k}^*)^{r_4/r_2}$, we have

$$\mathrm{sig}(x_{i1})^{\frac{2r_3-r_2}{r_1}}(x_{i2k} - x_{i2k}^*) \le 2^{1-\frac{r_2}{r_4}}\frac{2r_3 - r_2}{r_3}|\xi_{i1k}|^{\frac{2r_3-r_2}{r_4}} + 2^{1-\frac{r_2}{r_4}}\frac{r_2}{2r_3}|\xi_{i2k}|^{\frac{2r_3}{r_4}} \tag{39}$$

Therefore, we have:

$$\begin{aligned} &\dot{V}_1 \le \sum_{i=1,2,3}\Upsilon(k_a, k_b)E_{ik}\left(\bar{\delta}_{ia}/(\bar{x}_{i1} + \bar{\delta}_{ia})^2 + \bar{\delta}_{ib}/(\bar{\delta}_{ib} - \bar{x}_{i1})^2\right) \\ &\left[\left(2^{1-\frac{r_2}{r_4}}\frac{2r_3 - r_2}{r_3} - \alpha_0\right)|\xi_{i1k}|^{\frac{2r_3}{r_4}} + 2^{1-\frac{r_2}{r_4}}\frac{r_2}{2r_3}|\xi_{i2k}|^{\frac{2r_3}{r_4}}\right] \end{aligned} \tag{40}$$

Step 2: Given the form of ξ_{i2k}, V_2 satisfies:

$$V_2 \le \sum_{i=1,2,3} \left|x_{i2k} - x_{i2k}^*\right| \left|\xi_{i2k}\right|^{\frac{2r_3}{r_4}} \le \sum_{i=1,2,3} 2\left(\left|\xi_{i2k}\right|^{\frac{2r_3+r_2}{r_4}} + \left|\xi_{i1k}\right|^{\frac{2r_3+r_2}{r_4}}\right) \quad (41)$$

The derivative of V_2 with respect to t is given by:

$$\dot{V}_2 \le \sum_{i=1,2,3} \frac{2r_3}{r_4} 2^{1-\frac{r_2}{r_4}} \left|\xi_{i2k}\right|^{\frac{2r_3+r_2}{r_4}-1} \left|\frac{\mathrm{dsig}\left(x_{i2k}^*\right)^{r_4/r_2}}{\mathrm{d}t}\right| + \mathrm{sig}\left(\xi_{i2k}\right)^{2r_3/r_4} \dot{x}_{i2k} \quad (42)$$

According to Lemma 4, the following inequality holds

$$\left|\frac{\mathrm{dsig}\left(x_{i2k}^*\right)^{r_4/r_2}}{\mathrm{d}t}\right| \le \rho_1 \left|\xi_{i1k}\right|^{1-\frac{r_2}{r_4}} + \rho_2 \left|\xi_{i2k}\right|^{1-\frac{r_2}{r_4}} \quad (43)$$

where $\rho_1 = \frac{r_4}{r_1}\left(\frac{r_4 - r_1}{r_4 - r_2}\alpha_0^{r_4/r_2} + \alpha_0^{(r_4+r_2)/r_2}\right)$, $\rho_2 = \frac{r_4}{r_1}\frac{r_2}{r_4 - r_2}\alpha_0^{r_4/r_2}$.

Substitute (43) into (42). Based on Lemma 4, we have

$$\dot{V}_2 \le \sum_{i=1,2,3} \rho_3 \left|\xi_{i1k}\right|^{\frac{2r_3}{r_4}} + \rho_4 \left|\xi_{i2k}\right|^{\frac{2r_3}{r_4}} + \mathrm{sig}\left(\xi_{i2k}\right)^{2r_3/r_4} \dot{x}_{i2k} \quad (44)$$

where $\rho_3 = 2^{1-\frac{r_2}{r_4}} \rho_1 \frac{r_4 - r_2}{r_4}$, $\rho_4 = 2^{1-\frac{r_2}{r_4}} \rho_1 \frac{2r_3 + r_2 - r_4}{r_4} + \frac{2r_3}{r_4} 2^{1-\frac{r_2}{r_4}} \rho_2$.

Step 3: The time derivative of V is deduced as:

$$\begin{aligned}\dot{V} \le & -\sum_{i=1,2,3} \Upsilon(k_a, k_b) E_{ik}\left(\frac{\bar{\delta}_a}{\left(\bar{x}_1 + \bar{\delta}_a\right)^2} + \frac{\bar{\delta}_b}{\left(\bar{\delta}_b - \bar{x}_1\right)^2}\right) + \sum_{i=1,2,3} \rho_3 \left|\xi_{i1k}\right|^{\frac{2r_3}{r_4}} \\ & \left[\left(-2^{1-\frac{r_2}{r_4}} \frac{2r_4 - r_2}{r_3} + \alpha_0\right)\left|\xi_{i1k}\right|^{\frac{2r_3}{r_4}} - 2^{1-\frac{r_2}{r_4}} \frac{r_2}{2r_3}\left|\xi_{i2k}\right|^{\frac{2r_3}{r_4}}\right] + \rho_4 \left|\xi_{i2k}\right|^{\frac{2r_3}{r_4}} + \mathrm{sig}\left(\xi_{i2k}\right)^{2r_3/r_4} \dot{x}_{i2k}\end{aligned} \quad (45)$$

For ease of deduction, here we define:

$$\begin{aligned}\rho_{i5} &= \Upsilon(\delta_a, \delta_b) E_{ik}\left(\frac{\bar{\delta}_{ia}}{\left(\bar{x}_{i1} + \bar{\delta}_{ia}\right)^2} + \frac{\bar{\delta}_{ib}}{\left(\bar{\delta}_{ib} - \bar{x}_{i1}\right)^2}\right)\left(-2^{1-\frac{r_2}{r_4}} \frac{2r_4 - r_2}{2r_3} + \alpha_0\right) - \rho_3 \\ \rho_{i6} &= \Upsilon(\delta_a, \delta_b) E_{ik}\left(\frac{\bar{\delta}_{ia}}{\left(\bar{x}_{i1} + \bar{\delta}_{ia}\right)^2} + \frac{\bar{\delta}_{ib}}{\left(\bar{\delta}_{ib} - \bar{x}_{i1}\right)^2}\right) 2^{1-\frac{r_2}{r_4}} \frac{r_2}{2r_3} + \rho_4\end{aligned} \quad (46)$$

Along the deduction lines in Wang Z., Liang B., Wang X. 2018, we can obtain that

$$\begin{aligned}\dot{V} \le & -\rho_{10} V_1^{\frac{r_3+r_1}{2r_3+r_2}} - \rho_{11} V_1^{\frac{2r_3+r_4}{2r_3+r_2}} - \rho_{12} V_2^{\frac{r_3+r_1}{2r_3+r_2}} - \rho_{13} V_2^{\frac{2r_3+r_4}{2r_3+r_2}} + \varpi_{i2} \\ & -\sum_{i=1,2,3} \mathrm{sig}\left(\xi_{i2k}\right)^{2r_3/r_4}\left(\frac{1}{\varepsilon_2(t) - \left|\xi_{i1k}\right|}\mathrm{sgn}\left(\xi_{i2k}\right) - \varsigma(t)\right)\end{aligned} \quad (47)$$

where $\varpi_i = \rho_0\left(1 - \psi\left(\xi_{i2k}\right)\right)\left(\left|\xi_{i1k}\right|^{\frac{2r_3+r_4}{r_4}} + \left|\xi_{i2k}\right|^{\frac{2r_3+r_4}{r_4}}\right)$,

$$\rho_{i7} = \left(-2^{1-\frac{r_2}{r_4}} \frac{2r_4 - r_2}{2r_3} + \alpha_0\right) - \rho_3 \Bigg/ \left(\Upsilon(\delta_a, \delta_b) E_{ik}\left(\frac{\bar{\delta}_{ia}}{\left(\bar{x}_{i1} + \bar{\delta}_{ia}\right)^2} + \frac{\bar{\delta}_{ib}}{\left(\bar{\delta}_{ib} - \bar{x}_{i1}\right)^2}\right)\right)$$

$$\rho_{i9} = \frac{1}{2}\rho_{i7}\left(\frac{\bar{\delta}_{ia}}{\left(\bar{x}_{i1} + \bar{\delta}_{ia}\right)^2} + \frac{\bar{\delta}_{ib}}{\left(\bar{\delta}_{ib} - \bar{x}_{i1}\right)^2}\right)\frac{\left|\xi_{i1k}\right|^{\frac{2r_3}{r_4}}}{\Upsilon(\delta_a, \delta_b)} \quad \rho_{12} = \frac{\rho_0}{2 + \frac{r_3 + r_1}{2r_3 + r_2}} \quad \rho_{13} = \frac{\rho_0}{2 + \frac{2r_3}{2r_3 + r_2}}$$

$$\rho_{10} = \min\left(\left(\frac{2r_3 + r_2}{r_1}\right)^{\frac{r_3+r_1}{2r_3+r_2}} \frac{4r_4 + r_1}{r_3 + r_1} \rho_{i9}^{\frac{r_3+r_1}{4r_3+r_1}}\right) \quad \rho_{11} = \min\left(\left(\frac{2r_3 + r_2}{r_1}\right)^{\frac{2r_3+r_4}{2r_3+r_2}} \frac{4r_4 + r_1}{2r_3 + r_4} \rho_{i9}^{\frac{2r_3+r_4}{4r_3+r_1}}\right)$$

With (41) and Lemma 6, it can be derived that

$$\begin{aligned}\dot{V} \le & -\rho_{13} 2^{\frac{2r_3+2r_1}{2r_3+r_2}} V^{\frac{r_3+r_1}{2r_3+r_2}} - \rho_{13} 2^{\frac{4r_3+2r_4}{2r_3+r_2}} V^{\frac{2r_3+r_4}{2r_3+r_2}} + \sum_{i=1,2,3} \varpi_{i2} \\ & + \sum_{i=1,2,3} \mathrm{sig}\left(\xi_{i2k}\right)^{2r_4/r_2}\left(-\frac{1}{\left|\xi_{i1k}\right| - \varepsilon_2(t)}\mathrm{sgn}\left(\xi_{i2k}\right) + \varsigma(t)\right)\end{aligned} \quad (48)$$

where $\rho_{13} = \min\left\{\rho_{10}, \rho_{11}, \rho_{12}, \rho_{13}\right\}$.

Since $\varepsilon_2(t_2) = \varepsilon_3 \ll 1$ holds, the absolute value of ξ_{i1k} will always be less than $\varepsilon_3(t)$ under sufficient control quantities. According to Lemma 2, the settling time T and convergence neighbourhood D_0 can be represented as

$$T \le t_2 + \frac{1}{\rho_{13}\left(1 - \frac{r_3 + r_1}{2r_3 + r_2}\right)} + \frac{1}{\rho_{13}\left(\frac{2r_3 + r_4}{2r_3 + r_2} - 1\right)} \quad (49)$$

$$D_0 = \left\{\lim_{t \to T} \boldsymbol{x} \middle| V(\boldsymbol{x}) \le \min\left[\begin{array}{l}\rho_{13}^{-\frac{1}{r_3+r_1}}\left(\sum_{i=1,2,3} \varpi_{i2} + \mathrm{sig}(\varepsilon_1)^{2r_4/r_2}\left(\begin{array}{l}-\frac{\mathrm{sgn}(\varepsilon_1)}{|\varepsilon_3| - \varepsilon_2(t)} \\ +\varsigma(t)\end{array}\right)\right)^{\frac{1}{r_3+r_1}}, \\ \sum_{i=1,2,3} \rho_{13}^{-\frac{1}{r_3+r_1}}\left(\sum_{i=1,2,3} \varpi_{i2} + \mathrm{sig}(\varepsilon_1)^{2r_4/r_2}\left(\begin{array}{l}-\frac{\mathrm{sgn}(\varepsilon_1)}{|\varepsilon_3| - \varepsilon_2(t)} \\ +\varsigma(t)\end{array}\right)\right)^{\frac{2r_3+r_2}{2r_3+r_4}}\end{array}\right]\right\} \quad (50)$$

By adjusting $\varepsilon_2(t)$ and ε_1, D_0 can be arbitrarily small. Therefore, the fixed-time convergence and high accuracy are both guaranteed by the proposed controller (35).

5. SIMULATION

In order to demonstrate the effectiveness of the proposed controllers, numerical simulation results are presented here. The parameters of VTVL RLVs in of Zhang L., Wei C., Wu R. (2018) are adopted. Control parameters are as follows:

$q_1 = 1.6,\ p_1 = 1,\ q_2 = 1,\ p_2 = 1.44,\ k_{11} = k_{12} = k_{13} = 17,\ \varepsilon_0 = 0.1\pi/180,\ \kappa = 1\pi/180$

$r_1 = 0.05,\ r_2 = 0.25,\ r_3 = 0.05,\ r_2 = 0.05,\ \rho_0 = 6.5,\ \alpha_0 = 1.2,\ \kappa = 1.5$

$$\left\{k_{ci}(t)\right\}_1^3 = \begin{cases}\frac{\pi}{9} - \frac{19.95\pi}{180}\sin\left(\frac{\pi t}{2}\right) & t < 1 \\ \frac{0.05\pi}{180}\sin\left(\frac{\pi t}{2}\right) & t \ge 1\end{cases} \qquad \varepsilon_2(t) = \begin{cases}\frac{\pi}{9} - \frac{19.95\pi}{180}\sin\left(\frac{\pi t}{2}\right) & t < 1 \\ \frac{0.05\pi}{180}\sin\left(\frac{\pi t}{2}\right) & t \ge 1\end{cases}$$

The constraints of angles are $\alpha_{\min} = -0.2^\circ$, $\alpha_{\max} = 10^\circ$, $\beta_{\min} = -0.2^\circ$, $\beta_{\max} = 2.2^\circ$, $\sigma_{\min} = 0.6^\circ, \sigma_{\max} = -0.05^\circ$. The initial parameters are $\alpha = 0^\circ$, $\beta = 0^\circ$, $\sigma = 0.5^\circ$, angular velocities p, q and r equal to zero. Simulation results presented in Figs. 1-3 reveal the high accuracy and fast convergence rate of the AIBLF-based fixed-time controllers. The constraints are not violated during the tracking process. Tracking errors in three channels are less than 0.1deg, and converge to the small residual of steady desired values within 2.1s.

To validate the efficiency of ADEBLF-based controller, attitude orders and initial states are set to be the same as those in the simulation of AIBLF. The predefined constraints are $E_{\alpha\min} = -0.2^\circ$, $E_{\alpha\max} = 10^\circ$, $E_{\beta\min} = -0.2^\circ$, $E_{\beta\max} = 2.2^\circ$, $E_{\sigma\min} = 0.6^\circ$, $E_{\sigma\max} = -0.05^\circ$.Simulation results are presented in Figs.4-6. The orange dot line and the blue dot line represent the upper bound and the lower bound. During the tracking process, the tracking errors are less than 0.1deg, and the constraints stay unviolated. The attack angle, sideslip angle and bank angle are driven to the small residual of desired values within 2.1s.

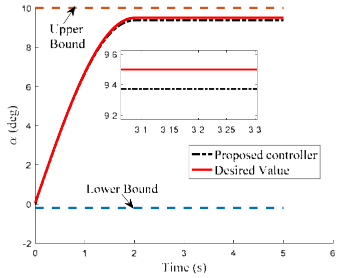

Figure 1 Time histories of attack angle under AIBLF-based control

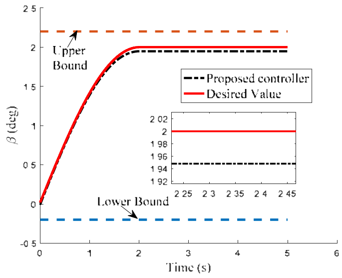

Figure 2 Time histories of sideslip angle under AIBLF-based control

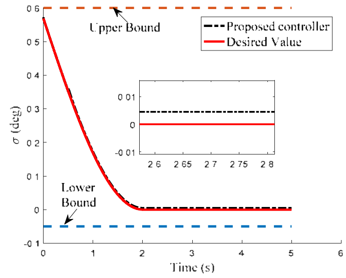

Figure 3 Time histories of bank angle under AIBLF-based control

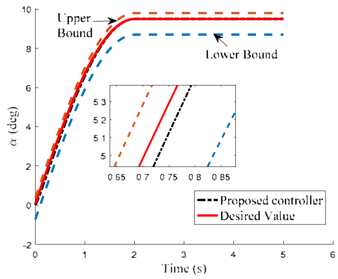

Figure 4 Time histories of attack angle under ADEBLF-based control

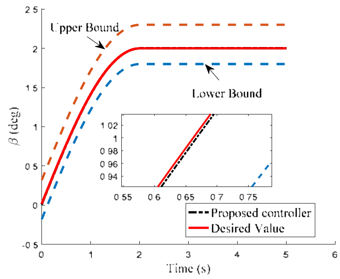

Figure 5 Time histories of sideslip angle under ADEBLF-based control

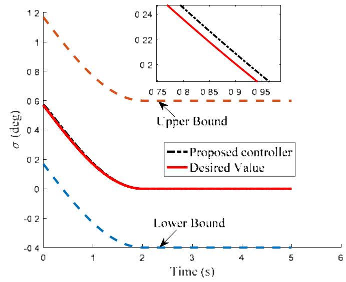

Figure 6 Time histories of bank angle under ADEBLF-based control

6. CONCLUSIONS

This paper proposes ALBLF and ADEBLF to deal with asymmetric constraints of VTVL RLVs in aerodynamic guidance phase. They both tend to infinity when the constrained states approach the boundary, while ADEBLF is of higher application value due to its continuity. Furthermore, practical fixed-time control laws based on two BLFs are derived, which guarantee that the order tracking errors converge to a small neighbourhood of the origin within a fixed time and constraints are not violated during the tracking process. Simulation results demonstrate the efficiency of the two proposed controllers.

REFERENCES

C.Z. Wei, X.Z. Ju, R. Wu, Y.F. He, Y. Diao (2019). Geometry and time updaters-based arbitrary-yaw iterative explicit guidance for fixed-thrust boost back of vertical take-off/vertical landing reusable launch vehicles, Aerospace Science and Technology. Published online.

Zhang, L., Wei, C., Wu, R., & Cui, N. (2018). Fixed-time extended state observer based non-singular fast terminal sliding mode control for a VTVL reusable launch vehicle. Aerospace Science and Technology, 82, 70-79.

Xu, B. (2015). Robust adaptive neural control of flexible hypersonic flight vehicle with dead-zone input nonlinearity. Nonlinear Dynamics, 80(3), 1509-1520.

An, H., Wang, C., & Fidan, B. (2017). Sliding mode disturbance observer-enhanced adaptive control for the air-breathing hypersonic flight vehicle. Acta Astronautica, 139, 111-121.

Wang, Z., Wu, Z., & Du, Y. (2016). Robust adaptive backstepping control for reentry reusable launch vehicles. Acta Astronautica, 126, 258-264.

Zhang, L., Wei, C., Wu, R., & Cui, N. (2019). Adaptive fault-tolerant control for a VTVL reusable launch vehicle. Acta Astronautica, 159, 362-370.

Blanchet, P., & Bartos, B. (2001). An improved load relief wind model for the Delta launch vehicle. Aerospace Sciences Meeting & Exhibit.

He, W., Dong, Y., & Sun, C. (2015). Adaptive neural impedance control of a robotic manipulator with input saturation. IEEE Transactions on Systems, Man, and Cybernetics: Systems, 46(3), 334-344.

Tee, K. P., Ge, S. S., & Tay, E. H. (2009). Barrier Lyapunov functions for the control of output-constrained nonlinear systems. Automatica, 45(4), 918-927.

Tee, K. P., & Ge, S. S. (2012, December). Control of state-constrained nonlinear systems using integral barrier Lyapunov functionals. In 2012 IEEE 51st IEEE Conference on Decision and Control (CDC) (pp. 3239-3244). IEEE.

Wang, X., Zhang, Y., & Wu, H. (2016). Sliding mode control-based impact angle control guidance considering the seeker′ s field-of-view constraint. ISA transactions, 61, 49-59.

He, W., Yin, Z., & Sun, C. (2016). Adaptive neural network control of a marine vessel with constraints using the asymmetric barrier Lyapunov function. IEEE transactions on cybernetics, 47(7), 1641-1651.

An, H., Xia, H., & Wang, C. (2017). Barrier Lyapunov function-based adaptive control for hypersonic flight vehicles. Nonlinear Dynamics, 88(3), 1833-1853.

Wang, Z., Sun, Y., & Liang, B. (2019). Synchronization control for bilateral teleoperation system with position error constraints: A fixed-time approach. ISA transactions.

Jiang, B., Hu, Q., & Friswell, M. I. (2016). Fixed-time attitude control for rigid spacecraft with actuator saturation and faults. IEEE Transactions on Control Systems Technology, 24(5), 1892-1898.